

The Journal of Physiology

<https://jp.msubmit.net>

JP-RP-2026-290221R1

Title: An age-associated decline in the role of the sarcoplasmic reticulum & associated calcium-handling proteins sets the pace for sinoatrial node function.

Authors: Sandra Jones
Fiona Godbeer
Matthew Lancaster

Author Conflict: No competing interests declared

Author Contribution: Sandra Jones: Conception or design of the work; Acquisition, analysis or interpretation of data for the work; Drafting the work or revising it critically for important intellectual content; Final approval of the version to be published; Agreement to be accountable for all aspects of the work Fiona Godbeer: Conception or design of the work; Acquisition, analysis or interpretation of data for the work; Drafting the work or revising it critically for important intellectual content; Final approval of the version to be published Matthew Lancaster: Conception or design of the work; Acquisition, analysis or interpretation of data for the work; Drafting the work or revising it critically for important intellectual content; Final approval of the version to be published

Running Title: Ageing causes calcium handling dysfunction in the SAN

Dual Publication: No

Funding: University of Hull (HU): Fiona S Godbeer, Studentship University of Hull funded a studentship for Dr Fiona Godbeer, previously known as Miss Fiona Hatch.

1
2 **An age-associated decline in the role of the sarcoplasmic**
3 **reticulum & associated calcium-handling proteins sets the**
4 **pace for sinoatrial node function.**
5

6 Running title: Ageing causes calcium handling dysfunction in the SAN
7

8

9 **Sandra A. Jones,* Fiona S. Godbeer* and Matthew K. Lancaster[†]**

10

11

12 *Centre for Biomedicine, Hull York Medical School, Faculty of Health Sciences, University of
13 Hull, Kingston-upon-Hull, HU6 7RX, UK and [†]School of Biomedical Sciences, Faculty of
14 Biological Sciences, University of Leeds, Leeds, LS2 9JT, UK.
15

16

17

18 ***Address for correspondence:***

19

20 Dr. Sandra A. Jones
21 Centre for Biomedicine, Hull York Medical School
22 Faculty of Health Sciences, University of Hull
23 Kingston-upon-Hull, HU6 7RX

24

25 Phone: + 441482 466463

26 E-mail: s.a.jones@hull.ac.uk

27

28

29

30 **Key Words:**

31 Ageing; arrhythmia; calcium; sarcoplasmic reticulum; sinoatrial node.

32

33 **Abbreviations:**

34 **βAR** - β adrenergic response, **BPM**, Beats per Minute, **Ca²⁺**, Calcium ions, **Ca_v1.2**, L-type
35 calcium channel, **CICR**, Calcium Induced Calcium Release, **CPA**, Cyclopiazonic acid, **CT**,
36 Crista terminalis, **LA** - Left atria, **NCX**, Sodium Calcium Exchanger, **PMCA** – Plasma
37 Membrane Calcium ATPase, **RA** - right atria, **RYR** – Ryanodine Receptor, **SAN** – Sinoatrial
38 node, **SERCA** – Sarcoendoplasmic reticulum Ca²⁺ ATPase, **SR** – Sarcoendoplasmic
39 reticulum

41 **Abstract**

42 With advancing age, the intrinsic function of the sinoatrial node (SAN) declines, due
43 to structural changes and changes in electrical regulation within the constitutive cells
44 of the nodal tissue. This study examined changes to proteins involved in regulating
45 calcium flux balance in the atria and SAN of male rats used as a model of ageing
46 throughout their lifespan at 6, 12 and 24 months of age. Using
47 immunohistochemistry and western blot, we determined a significant age-dependent
48 decline in the levels of key calcium regulatory proteins within the SAN: $\text{Ca}_v1.2$,
49 PMCA4, RYR2, SERCA2a, and phospholamban ($n=5$; ANOVA; $p<0.05$). In contrast,
50 levels of NCX protein were significantly elevated by 57.3% ($p = 0.009$) in the oldest
51 group indicating a potential pronounced change in calcium balance; a difference
52 functionally observed by a steeper dose-response curve to the inhibitory effects of
53 nifedipine. Intrinsic pacemaker beating rate was significantly reduced by 68 beats
54 per minute in the oldest group compared with the youngest, ($n = 6$; ANOVA $p =$
55 0.022). Negating sarcoplasmic reticulum calcium cycling and the 'calcium clock'
56 using cyclopiazonic acid reduced the intrinsic pacemaker activity of the SAN in
57 young animals to that observed in the oldest group. Under these conditions,
58 spontaneous activity and response of the SAN to isoprenaline became matched
59 across all age groups. Restoring sarcoplasmic reticulum function to the SAN in the
60 elderly may offer a route to combatting age-related suppression of function, but care
61 should be taken in the use of calcium channel antagonists to avoid precipitating sick-
62 sinus syndrome.

63

64 **Key Points:**

- 65 • This study adds understanding and characterisation of the age-dependent progressive
66 reduction in sinoatrial node (SAN) function.
- 67 • We compared atria and the sinoatrial node across the lifespan of a Han-Wistar rat
68 model of ageing with animals studied at 6, 12 and 24 months of age.
- 69 • Sinoatrial node tissue from old rats showed significantly reduced expression of key
70 cellular calcium regulatory proteins compared with nodal tissue from young rats.
- 71 • The sinoatrial node from old rats exhibited a slowed intrinsic beating rate and an
72 altered response to drugs that modulate cellular calcium handling.
- 73 • Eliminating sarcoplasmic reticulum calcium handling makes the sinoatrial node of a
74 young animal mimic features of an aged animal.

75

76 **Abstract Figure legend**

77 Stable, responsive pacemaking in the sinoatrial node is driven by the activity of the funny
78 current (membrane clock), interplay of calcium cycling and release from the
79 sarcoendoplasmic reticulum with depolarising sodium-calcium exchange current (calcium
80 clock). With increasing age key proteins associated with calcium cycling are reduced limiting
81 the role of the calcium clock and it's ability to deal with situations that exacerbate calcium
82 buffering requirements such as adrenergic stimulation and modulation of calcium channels.
83 The net effect is an increasing risk of sinoatrial node instability and dysfunction with ageing.

84

85 **Introduction**

86 The sinoatrial node (SAN) is a spontaneously active, heterogeneous region of tissue located
87 within the intercaval region of the right atrium of the heart serving as the heart's primary
88 pacemaker. The intrinsic automaticity of the SAN and responsiveness to β -adrenergic
89 stimulation declines in an age-correlated manner contributing to a reduction in functional
90 capacity and ability to respond to stress, as well as potentially increasing risk of arrhythmias
91 such as atrial fibrillation in later life (Turner *et al.*, 1999; Fleg *et al.*, 2005; Fang *et al.*, 2007).
92 Within 20 years it is estimated over a third of the UK population will be ≥ 65 years of age with
93 $> 10\%$ diagnosed with atrial arrhythmias, (ONS, 2025) resulting in spiralling NHS costs
94 (Burdett & Lip, 2022). The onset of such arrhythmias is particularly pronounced in males
95 where the impact seems to become evident at an earlier age so this group has been the
96 initial focus of our study (Keller & Howlett, 2016). The aim of this study was to add to our
97 knowledge of the age-dependent progressive deterioration in SAN function in order to
98 identify mechanisms predisposing to rising dysfunction and risk of arrhythmias, with potential
99 routes to preventative and direct treatment.

100

101 An unstable membrane voltage drives pacemaking within SAN myocytes. Hyperpolarisation-
102 activated ion channels pass depolarising I_f current contributing to spontaneous
103 depolarisation of SAN myocytes, supplemented in the late phase of diastole by spontaneous
104 releases of calcium from the sarcoplasmic reticulum (SR) (Bers & Lakatta, 2023). These
105 calcium releases drive a small amount of sodium calcium exchange current (I_{NCX}) enhancing
106 the rate of depolarisation to the membrane threshold for triggering a full action potential. This
107 latter component of depolarisation is referred to as the 'calcium clock' and complements the
108 overall 'membrane 'clock' in ensuring a robust capability for the heart rate, as driven by the
109 SAN, to respond dynamically to stress. As such it is recognised that the balance of calcium
110 ion flux both across the cell membrane and within the sarcoplasmic reticulum of the cells of
111 the SAN is a key component controlling SAN pacemaker function (Yue *et al.*, 2020; Bers &
112 Lakatta, 2023).

113

114 Adrenergic stimulation predominantly increases the heart rate directly or indirectly by
115 causing elevations in cAMP. Numerous components key to SAN function are sensitive to
116 cAMP and its actions in either directly changing ion-channel kinetics (e.g. by enhancing
117 activation of I_f) or subsequently by its impact on calcium regulation (e.g. by increasing
118 calcium loading of the SR by alterations to phospholamban and the calcium current as well
119 as the overall action potential)(Tsutsui *et al.*, 2018; Bers & Lakatta, 2023). We have
120 previously shown that pacemaker cells from the Guinea Pig SAN show an age-associated

121 decline in $\text{Ca}_v1.2$ protein expression, (Jones *et al.*, 2007) which is key to potentially limiting
122 depolarisation of the cells but also can reduce calcium-loading of the SR and so modulate
123 the calcium clock. We have now sought to track age-associated changes in other key
124 calcium handling proteins that impact the SAN 'calcium clock' as we aim to further
125 understand age-related changes in the basal function of the SAN and response to
126 adrenergic stimulation. Our study hypothesis was that a reduced basal beating rate and
127 dynamic response to adrenergic stimulation in the SAN of aged individuals is due to a
128 reduced capacity for dynamic response of the 'calcium clock' limiting its ability to facilitate
129 cardiac acceleration.

130

131

132 **Materials and Methods**

133 **Ethical approval**

134 In accordance with our Institution's animal welfare committee guidelines animals had free
135 access to water and food, appropriate housing, and were monitored to ensure they were
136 healthy and displayed normal daily activities. Animals were euthanised by anaesthetic
137 overdose (Euthatal - Sodium Pentobarbital i.p.), and death confirmed. All animal
138 experimental procedures were performed in accordance with Home Office UK guidelines
139 (United Kingdom Animals (Scientific Procedures) Act, 1986) with ethical review and approval
140 from the local ethics committee (reference number, UoH U002).

141

142 **Sinoatrial node isolated from rats.**

143 Male Han-Wistar rats (Charles River, UK) fed standard chow were randomised to differing
144 age categories and raised to their appropriate age in caged social groups. Our rat model of
145 ageing examined rats across their lifespan at the ages of 6 (young), 12 and 24 (old) months.
146 Animals were euthanised at the appropriate age and the heart rapidly excised and immersed
147 in oxygenated Tyrode solution with 95 % O₂/5 % CO₂, pH 7.4, 37°C. For experiments
148 involving mapping the activity of the SAN the right atrium dissected from the heart and
149 opened to expose the intercaval region and nodal tissue (Jones *et al.*, 2004). Tissue
150 architecture defined the SA node tissue as detailed in figure 1.

151

152 **Figure 1. Endocardial surface of the right atria**

153 Flanked by the right atrial appendage muscle and septum tissue, the dashed lines indicate
154 location of the crista terminalis (CT) and sinoatrial (SA) node tissue regions, between the
155 upper the superior vena cavae (SVC) and lower inferior vena cavae (IVC). Scale bar, 5mm
156

157 **Extracellular electrode recordings**

158 We used our published approach for recording sites of initiation and spread of activity across
159 the SAN (Jones *et al.*, 2004). Extracellular bipolar electrodes were positioned on the SAN
160 leading pacemaker site (earliest point of activation) and pectinate muscle of the
161 neighbouring right atrial tissue (Fig. 1) to record nodal activation (Neurolog bridge amplifier
162 (Digitimer, UK); Digidata Axon 1440A with Clampex 10 (Molecular devices, UK)) and
163 determine the intrinsic heart rate (IHR). Movement of one of the electrodes in 1 mm steps
164 across the x and y ranges of the tissue permitted a full map of activation timing to be
165 produced across the tissue. Oxygenated Tyrode solution maintained the tissue at a flow rate
166 of 40ml/min with temperature monitored and controlled at 37 °C. The kinetics of pacemaking

167 are sensitive to temperature so it is important for close regulation (+/- 0.5 degrees) to ensure
 168 stable pacemaking in the normal physiological range. Pharmacological agents, isoprenaline
 169 hydrochloride, nifedipine and cyclopiazonic acid (CPA) (Sigma-Aldrich) were made to 1
 170 mM/L stock solutions before dilution to the required concentration in Tyrode solution. For
 171 each drug dose the preparation was perfused for a minimum of 15 minutes to allow
 172 equilibration and to establish the steady-state IHR prior to recording. All chemicals were
 173 purchased from Merck Life Science UK Limited.

174

175 **Analysis of protein expression**

176 Using our previously published method (Jones *et al.*, 2004), tissue was frozen, and a lysate
 177 produced for western blot (WB). Proteins were separated using SDS-PAGE, transferred to
 178 PVDF and incubated overnight at 4°C with the primary antibodies at 1:1000 dilution followed
 179 for 1 hour by incubation with the appropriate secondary antibody conjugated to HRP (Dako,
 180 UK) (Table 1). A Bio-Rad Molecular Imager Chemi Doc XRS+ was used to image band
 181 densities and associated values determined using ImageJ 1.54g (NIH, USA). Density values
 182 were normalised to an appropriate housekeeper protein to control for equal protein loading
 183 per sample.

184

185 **Table 1. Primary antibodies.**

Protein	Cat. No.	Company	Country	Primary host	Secondary antibody
Ca_v1.2	ACC-003	Alomone Labs	Israel	Rabbit	Swine Anti-rabbit
Ca_v1.3	ACC-005	Alomone Labs	Israel	Rabbit	Swine Anti-rabbit
Ca_v3.1	ACC-021	Alomone Labs	Israel	Rabbit	Swine Anti-rabbit
SERCA2	MA3-910	Thermo Scientific	UK	Mouse	Rabbit anti-mouse
PMCA4	MA1-914	Thermo Scientific	UK	Mouse	Rabbit anti-mouse
RYR2	MA3-916	Thermo Scientific	UK	Mouse	Rabbit anti-mouse
NCX1	MA3-926	Thermo Scientific	UK	Mouse	Rabbit anti-mouse
PLB	A010	Badrilla	UK	Mouse	Rabbit anti-mouse
Desmin	M 0760	Dako	Denmark	Mouse	Rabbit anti-mouse

186

187 As previously described for immunohistochemistry (IHC) (Jones *et al.*, 2004), 10µm frozen
 188 tissue slices were incubated overnight at 4°C with the primary antibodies (1:250 dilution,
 189 except for that for PLB which was used at 1:100). Tissue was incubated for 2 hours with a
 190 secondary antibody conjugated to Alexa Fluor™ 488 antibody and wheat germ agglutinin
 191 conjugated to rhodamine (2BScientific, UK). Labelled proteins were imaged using a plan
 192 apochromat 40x/1.3 oil iris M27 lens on a LSM 710 confocal with images captured using Zen
 193 software 3.12 (Zeiss Microscopy, Ltd.; U.K.). Images were processed within the Zen software
 194 to allow separation of the fluorescent channels corresponding to the two labels before
 195 performing densitometric assessment of fluorescence intensity for regions. To control for

196 background signal an unlabelled parallel section of tissue from the sample was also
197 measured using the same approach and the result subtracted. For the protein of interest IHC
198 labelling was collected on the same settings across each age group. Levels of fluorescent
199 labelling are shown in some cases normalised relative to the mean value as determined in
200 tissue from animals at 6 months of age.

201

202 **Quantitative polymerase chain reaction (QPCR)**

203 We used the RNeasy Fibrous Tissue Mini Kit (Qiagen) to extract mRNA from samples of the
204 rat right atria. Extracted mRNA concentration was assessed by absorbance (NanoDrop
205 1000) prior to performing qPCR. Reverse transcriptase (Invitrogen U.K) reverse transcribed
206 RNA to complementary DNA (cDNA). Samples of cDNA were stored at 2-4°C for a
207 maximum of 3 days. We detected the cDNA within each sample using a sequence-specific
208 DNA probe. Primers were Desmin (rat NM_022531.1) and GAPDH (rat NM_017008.3) from
209 Invitrogen UK. Transcript primers were optimised to ensure a cycle threshold (CT) value of
210 29 or less, confirming a strong positive reaction indicative of abundant target nucleic acid. An
211 Applied Biosystems StepOne Plus qPCR machine was used with StepOne software:QPCR
212 to quantify expression in each sample.

213

214 **Statistics:**

215 Data are presented as mean \pm SD. Statistical significance was evaluated by Student's t-test,
216 One-way ANOVA or two-way repeated-measures (RM) ANOVA with Holm-Sidak post-hoc
217 comparisons as appropriate. Alternatively, a Kruskal-Wallis comparison was used where
218 required and indicated. P<0.05 was taken as statistically significant. Curve fits and statistical
219 analysis were performed in GraphPad Prism 10 or Excel as appropriate. Unless otherwise
220 stated, n = number of animals. Data, where appropriate, is shown relative to that obtained
221 from samples from the youngest age group at 6 months of age. For protein analysis it is
222 taken that the 6 months age group possessed 100 % of the specific protein of interest to
223 enable calculation of % change relative to that age point.

224

225 **Results**

226

227 **Age-associated changes in morphological characteristics**

228 We compared tissue obtained from healthy male rats across three age groups: 6, 12 and 24
 229 months of age (Table 2). Data showed rat body weight gradually increased in an age-
 230 correlated manner ($r^2 = 0.3966$; $p = 0.0003$ by linear regression). A comparison of rats aged
 231 6 and 24 months revealed a significant increase in body weight from 517 ± 35 g to 661 ± 125
 232 g ($n = 11$; $p = 0.000772$) as body weight significantly increased between the ages of 6 and
 233 12 months ($p = 0.0416$), 12 and 24 months ($p = 0.0120$). In contrast heart weight did not
 234 change significantly from 1.55 ± 0.20 g across the age groups of 6, 12 and 24 months (Table
 235 2; ANOVA $p = 0.375$).

236

237 Rats of 6 months and 12 months of age exhibited no significant difference in their heart-to-
 238 body weight ratio (ratio of 6-month rat $2.94 \pm 0.33 \times 10^{-3}$; $n = 6$; t-test $p = 0.244$). Whereas
 239 rats aged 24 months revealed a significant reduction in their heart-to-body weight ratio ($2.5 \pm$
 240 0.27×10^{-3}) when compared with the other age groups of 6 months and 12 months (Table 2;
 241 $n = 11$; 24 vs 6 months ANOVA; $p = 0.000481$; 24 vs 12 months $p = 0.000113$).

242

243 **Table 2. Morphological characteristics of the ageing rat model.**

	6 months	12 months	24 months
Body weight (g)	517 ± 35	556 ± 40	661 ± 125 *
Heart weight (g)	1.55 ± 0.20	1.64 ± 0.07	1.63 ± 0.18
Heart: Body ($\times 10^{-3}$)	2.94 ± 0.33	2.96 ± 0.10	2.5 ± 0.27 ▶¥
Number in group (n)	11	6	11

244 * $p=0.000772$, 24 months compared with 6 months of age.

245 ▶ $p= 0.000481$, 24 months compared with 6 months of age.

246 ¥ $p= 0.000113$, 24 months compared with 12 months of age.

247

248

249

250 **Conforming a suitable housekeeper reference for our ageing studies**

251 We determined mRNA expression of the muscle-specific protein desmin and metabolic
 252 enzyme Glyceraldehyde 3-phosphate dehydrogenase (GAPDH) for variance with increasing
 253 age (Table 3) using our qPCR protocol. Maximum cycle threshold (C_T) differences in the
 254 right atrial tissue for desmin RNA was 0.3 C_T with no significant changes over the examined
 255 age range (n = 5; ANOVA p = 0.314), whereas GAPDH significantly reduced by 1.0 C_T with
 256 ageing (n = 5; ANOVA, 6 vs 24 months p = 0.024; 12 vs 24 months p = 0.021). We also
 257 examined desmin protein levels in paired right atrial (RA) and left atrial (LA) tissue obtained
 258 from rats at 6, 12 and 24 months of age: There was no significant change in desmin levels (n
 259 = 5; ANOVA, p = 0.691), thus desmin was used as the reference housekeeper protein for
 260 western blotting in this study.

261

262 **Table 3. Desmin and GAPDH RNA values in right atrial tissue from rats of increasing**
 263 **ages.**

Animal age (months)	RNA C_T values (Mean \pm SD)	
	Desmin	GAPDH
6	23.6 \pm 0.45	21.8 \pm 0.55
12	23.9 \pm 0.35	21.8 \pm 0.49
24	23.6 \pm 0.47	20.8 \pm 0.35

264

265 **Table 4. Desmin protein density**

Animal age (months)	Tissue type	Desmin protein (Density/pixel)
6	Left atria	3.15 \pm 0.25
12	Left atria	3.12 \pm 0.19
24	Left atria	3.88 \pm 0.58
6	Right atria	3.53 \pm 0.71
12	Right atria	2.83 \pm 0.40
24	Right atria	3.00 \pm 0.59

266

267 **Age-associated changes in calcium channels in the rat right atria**

268 Immunohistochemistry (IHC) as performed on RA tissue from rats aged 6 and 24 months,
269 showed age-associated changes in the proteins $\text{Ca}_v1.2$, $\text{Ca}_v1.3$ and $\text{Ca}_v3.1$ (Fig. 2).
270 Normalised to the young, the old rat $\text{Ca}_v1.2$ protein levels significantly declined to $50.2 \pm$
271 4.72% , whereas $\text{Ca}_v1.3$ and $\text{Ca}_v3.1$ levels increased by $81.6 \pm 10.14\%$ and $43 \pm 23.42\%$
272 respectively (mean \pm S.D.; ANOVA; $p = 0.0001$).

273

274 **FIGURE 2 BELONGS HERE**

275

276 **Figure 2. Changes in IHC calcium channel label within RA at 24 months of age.**

277 **A**, optical slices of RA tissue from rats at 6 and 24 months of age with fluorescent labelling of
278 $\text{Ca}_v1.2$, $\text{Ca}_v1.3$ and $\text{Ca}_v3.1$. Confocal images, scale bar = $20 \mu\text{m}$. **B**, data shown as mean (\pm S.D.)
279 difference per calcium channel, overlaid with raw data points. Where n = rats per group, $\text{Ca}_v1.2$ (n
280 = 10), $\text{Ca}_v1.3$ (n = 5) and $\text{Ca}_v3.1$ (n = 9) with statistically significant changes in each case relative
281 to that seen in tissue from young animals (ANOVA; $p = 0.0001$).

282

283

284

285

286 **Age-associated changes in Cav1.2 protein levels across the rat atria**

287 RA and LA tissue from rats aged 6, 12 and 24 months were analysed by western blot (Fig.
288 3). $\text{Ca}_v1.2$ protein levels in the RA showed a significant drop with increasing age to $53.6 \pm$
289 14.1% of that in the young ($n = 5$; ANOVA, $p = 0.011$), but in the LA no significant change in
290 expression was seen ($p = 0.051$).

291

292 **FIGURE 3 BELONGS HERE**

293

294 **Figure 3. Age-associated changes of $\text{Ca}_v1.2$ protein across the atria.**

295 **A**, Illustrative blot of $\text{Ca}_v1.2$ protein levels per age group for both the RA and LA. **B**, data shown as
296 mean \pm S.D. per age group, overlaid with raw data points. ($n = 5$ animals at each age; ANOVA, * p
297 = 0.011 for 24 vs. 6 months).

298

299 **Age-dependent decline in $\text{Ca}_v1.2$ ion channel expression in the sinoatrial node**

300 Western blot analysis of $\text{Ca}_v1.2$ channel protein expression within the SAN of rats at 12
301 months of age showed no significant differences to that found in the node of those aged 6
302 months ($100 \pm 24.4\%$; Fig. 4A; ANOVA $p = 0.207$). At 24 months though $\text{Ca}_v1.2$ expression
303 levels had significantly declined to $59.6 \pm 18.6\%$ of that observed in the 6 months age group
304 (Fig. 4A; ANOVA, 12 vs 24 months $p = 0.004$, 6 vs 24 months $p=0.0315$). We observed a
305 striated pattern by IHC $\text{Ca}_v1.2$ protein labelling within SAN tissue in all age groups, however
306 the amount of labelled protein observed significantly declined from 6 months ($100 \pm 2.2\%$)
307 to $55.6 \pm 5.8\%$ at 24 months of age (Fig. 4B; $p = 2.53 \times 10^{-7}$). Data therefore consistently
308 shows a substantial age-dependent decline of $\text{Ca}_v1.2$ protein expression within the SAN
309 region in hearts once animals reach 24 months of age compared with that identified within
310 the young age group (6 months).

311

312 **Modulation of $\text{Ca}_v1.2$ function and activity of the sinoatrial node**

313 The intrinsic heart rate of the isolated SAN was assessed and impact of blockade of $\text{Ca}_v1.2$
314 channels determined by application of the selective channel blocker nifedipine across a dose
315 range of $0.1\mu\text{M}$ - $30\mu\text{M}$. Dose-response relationships for nifedipine's actions in each age
316 group were established using a Hill curve to fit the intrinsic heart rate data and the nifedipine
317 dose, plotted using a standard \log_{10} scale for each concentration trialled (Fig. 4C). The SAN
318 from the youngest age group of 6 months showed a dose-dependent response to nifedipine
319 with Hill slope coefficient of 0.94; the maximum dose of $30\mu\text{M}$ nifedipine caused all
320 spontaneous activity to cease. The SAN from the oldest age group of 24 months had a
321 reduced response to $0.1\mu\text{M}$ nifedipine, $0.3\mu\text{M}$ caused a dramatic decline in beating rate with
322 complete cessation at $1\mu\text{M}$ nifedipine. The dose-response relationship in the nodes from
323 animals at 24 months of age had an average Hill slope coefficient of 4.2. The IC₅₀ for
324 nifedipine in the older age group was not significantly different to that seen in the young
325 (IC₅₀; $1.14\mu\text{M}$ at 6 months vs. $1.23\mu\text{M}$ at 24 months). Therefore, although the inhibitory
326 binding of nifedipine for $\text{Ca}_v1.2$ is comparable for each age group, the impact on beating rate
327 within the old age group has an approximate four-fold steeper relationship than that seen at
328 a young age.

329

330 **FIGURE 4 BELONGS HERE**

331

332 **Figure 4. Age-associated changes of $\text{Ca}_v1.2$ protein and activity within the SAN.**

333 **A**, Illustrative blot of $\text{Ca}_v1.2$ protein levels in the RA at 6, 12 and 24 months. Data shown as mean
334 \pm S.D. with raw data points. ($n = 5$ per group; 12 vs 24 months $p = 0.004$, 6 vs 24 months $p =$

335 0.0315 by ANOVA). **B**, optical slices from SAN of rats aged 6 and 24 months with $\text{Ca}_v1.2$ protein
336 labelled in green and membranes labelled with wheat germ agglutinin (red). Scale bar = 50 μm .
337 Quantitated labelling density per group with raw data is shown below. (mean \pm S.D.; n = 5 animals
338 per age group; 6 vs 24 months $p = 2.53 \times 10^{-7}$ ANOVA); **C**, Hill equation fitted to intrinsic heart rate
339 from rats aged 6 months and 24 months with incrementing concentrations of nifedipine (shown as
340 \log_{10}). (n = 6 per group; IC50 = 1.14 μM at 6 months vs. 1.23 μM at 24 months).
341
342

343 **Age-dependent changes of calcium handling protein within the sinoatrial node**

344 Faced with a reduced capacity for calcium influx it is reasonable to expect extrusion
345 pathways may be modulated to maintain calcium balance in nodal tissue from elderly
346 animals. Intracellular balance of Ca^{2+} is maintained by extrusion via sodium-calcium
347 exchanger (NCX1) and plasma membrane calcium ATPase 4 (PMCA4) with
348 sarcoendoplasmic reticulum Ca^{2+} ATPase2a (SERCA2a) maintaining internal calcium
349 buffering by pumping calcium back into the SR store although this is modulated by the
350 inhibitory action of phospholamban (PLB).

351

352 Analysed by western blotting NCX1 protein levels within the SAN did not alter significantly
353 between the ages 6 to 12 months, but in rats aged 24 months NCX1 levels were significantly
354 increased to 157 ± 21.5 % of that found in tissue from the 6-month group with levels also
355 being elevated significantly relative to that seen at 12 months too (Fig. 5B; 12 vs 24 months
356 $p = 0.024$, 6 vs 24 months $p = 0.00856$; ANOVA). Analysis of immunolabelling of NCX1
357 protein within the SAN region identified a similar significant rise with age to 142 ± 15.6 % at
358 24 months compared with 100 ± 12.8 % at 6 months of age (Fig. 6; $p = 0.0008$). Using
359 western blot we identified PCMA4 calcium pump protein levels within the SAN increased
360 significantly from 6 to 12 months to 122 ± 17.4 % but exhibited a significant decline to $78 \pm$
361 3.0 % of the amount at 6 months in rats aged 24 months (Fig. 5C; 6 vs 12 months $p = 0.029$;
362 12 vs 24 months $p = 0.002$; 6 vs 24 months $p = 0.010$). IHC labelling of PCMA4 within the
363 SAN region also showed a similar significant decline with age to 76.9 ± 16.3 % at 24 months
364 compared with 100 ± 11.1 % at 6 months of age (Fig. 6; $p = 0.0157$).

365

366 Both ryanodine receptor 2 (RYR2) and SERCA2a also showed significant changes in
367 expression with age. Western blot showed the RYR2 protein levels rose significantly to 135
368 ± 18.8 % within the SAN from rats aged 12 months compared with tissue from those aged 6
369 months, but then in rats aged 24 months levels significantly declined to 68 ± 23.2 % of the
370 level in tissue from rats at 6 months of age (Fig. 5D; 6 vs 12 months $p = 0.014$, 12 vs 24
371 months $p = 0.0005$; 6 vs 24 months $p = 0.029$). IHC labelling of RYR2 protein within the SAN
372 region also showed a significant decrease to 72.6 ± 13.4 % at 24 months compared with 100
373 ± 13.7 % at 6 months of age ($p = 0.006$). SERCA2a levels significantly increased to $144 \pm$
374 39.4 % within the SAN from rats aged 12 months compared with those aged 6 months but
375 then declined significantly to 64 ± 14.7 % in tissue from rats at 24 months of age (Fig. 5E; 6
376 vs 12 months $p = 0.035$, 12 vs 24 months $p = 0.003$; 6 vs 24 months $p = 0.002$). IHC
377 labelling of SERCA2a within the SAN region also showed a significant decrease with age to
378 71.7 ± 15.3 % at 24 months compared with 100 ± 14.3 % at 6 months of age (Fig. 6; $p =$
379 0.008).

380
381
382 **FIGURE 5 BELONGS HERE**
383

384 **Figure 5. Effect of ageing on levels of calcium handling proteins expressed in the**
385 **sinoatrial node. A**, illustrative western blot of nodal tissue examined for each protein of
386 interest per age group with the desmin housekeeper. **B-D**, Mean \pm S.D. per age group (n = 5
387 animals per group) overlaid with raw data points for nodal expression levels of calcium
388 handling proteins; **NCX1** (5B; ANOVA 12 vs 24 months *p = 0.024, 6 vs 24 months $^{\#}$ p =
389 0.00856), **PMCA4** (5C; ANOVA 6 vs 12 months *p = 0.029; 12 vs 24 months $^{\Delta}$ p = 0.002; 6
390 vs 24 months $^{\#}$ p = 0.010), **RYR2** (5C; ANOVA 6 vs 12 months *p = 0.014, 12 vs 24 months
391 $^{\Delta}$ p = 0.0005; 6 vs 24 months $^{\#}$ p = 0.029), and **SERCA2A** (5E; 6 vs 12 months *p = 0.035, 12
392 vs 24 months $^{\Delta}$ p = 0.003; 6 vs 24 months $^{\#}$ p = 0.002).

393
394
395 **FIGURE 6 BELONGS HERE**

396
397
398 **Figure 6. Age-dependent changes of proteins labelled within the sinoatrial region.**
399 **A**, optical slice of each section taken through the sinoatrial node regions from rats aged 6 and
400 24 months were labelled to show expression of specific proteins of interest (green), and all
401 membranes (using wheat germ agglutinin, red). Confocal images scale bar = 50 μ m. **B**,
402 quantified fluorescence from IHC expressed relative to signal density from labelled sections of
403 nodal tissue from rats at 6 months of age (Mean \pm S.D.; n=5 animals; Student's t-test, NCX1 *
404 p = 0.0008; PMCA4 $^{\Delta}$ p = 0.0157; RYR2 $^{\#}$ p = 0.006, SERCA2A $^{\diamond}$ p = 0.008. and total PLB \spadesuit p =
405 0.035.

406

407 **Age-dependent changes in expression of phospholamban in the sinoatrial node.**

408 PLB is expressed as monomer but can dynamically establish a pentameric assembly which
 409 disassembles upon phosphorylation in response to adrenergic stimulation whereupon the
 410 monomeric form serves as a more effective regulatory inhibitory protein modulating SERCA
 411 pump activity (MacLennan & Kranias, 2003). We quantified monomeric PLB protein levels
 412 within the SAN (Fig. 7B) and these did not significantly alter between the ages of 6 and 12
 413 months ($p = 0.38$). Monomeric PLB expression however significantly fell in SAN tissue from
 414 rats aged 24 months to $58.6 \pm 11.3\%$, with this fall being significant when compared with
 415 levels in SAN from rats at 6 and 12 months of age ($n = 5$; 6 vs. 24 months, $p = 0.0016$; 12
 416 vs. 24 months, $p = 0.0017$).

417

418 By comparison pentameric PLB protein levels rose from $100 \pm 20.8\%$ at 6 months to $119.1 \pm 22.3\%$ at 12 months of age ($p = 0.09$), then in rats aged 24 months significantly declined
 419 to $72.4 \pm 21.0\%$ (Figure 7C, 12 vs. 24 months $p = 0.004$; 6 vs. 24 months $p = 0.035$). Total
 420 PLB levels did not alter from 100% between the ages 6 to 12 months ($p = 0.47$) but
 421 significantly decreased to $68.9 \pm 19.3\%$ in rats aged 24 months (Figure 7D, 12 vs. 24
 422 months $p = 0.0120$; 6 vs. 24 months $p = 0.0123$). This age-dependent decrease between
 423 young and old rats was also observed in our total PLB protein immunolabelling of the SAN,
 424 as label density significantly fell from 6 months ($100 \pm 16.5\%$) to $78.7 \pm 15.7\%$ at 24 months
 425 (Figure 6, 6 vs. 24 months, $p = 0.035$). The ratio of SERCA pump protein to PLB monomer
 426 (SERCA : PLB) is considered indicative of activity and was determined as 1.0 ± 0.31 at 6
 427 months and significantly rose at 12 months to 1.5 ± 0.148 , indicative of greater tonic SERCA
 428 inhibition (Fig. 7E; 6 vs. 12 months $p = 0.0080$). From 12 months onwards the SERCA : PLB
 429 ratio declined significantly to 1.2 ± 0.17 at 24 months (12 vs. 24 months $p = 0.0125$). The
 430 SERCA : PLB ratio observed in tissue from rats aged 6 months was not significantly different
 431 to that observed in 24 months aged animals ($p = 0.10$).

432

433

434

FIGURE 7 BELONGS HERE

435

436 **Figure 7. Age-dependent protein expression changes of phospholamban in the**
 437 **sinoatrial node.**

438 **A-D**, Illustrative western blot and protein levels per age group of total PLB, alongside
 439 separated data for pentameric and monomeric forms normalised to desmin. Mean \pm S.D.; n
 440 = 5; ANOVA. Protein levels declined in SA nodes from rats age 24 months for B monomer
 441 PLB protein levels (6 vs. 24 months, $^*p = 0.0016$; 12 vs. 24 months, $^{\#}p = 0.0017$), C
 442 pentamer PLB protein levels (12 vs. 24 months $^*p = 0.004$; 6 vs. 24 months $^{\#}p = 0.035$) and
 443 D total PLB protein levels (6 vs. 24 months $^*p = 0.0123$; 12 vs. 24 months $^{\#}p = 0.0120$). E,

444 The SERCA : PLB ratio protein levels increased in SA nodes from rats at 12 months of age,
445 then decline back to the 6 months rat levels (6 vs. 12 months *p = 0.0080;12 vs. 24 months
446 [#]p = 0.0125; 6 vs 24 months, p = 0.10).

447

448

449 **Age dependent decline in SERCA2a activity of the SAN and pacemaker**
 450 **dynamics.**

451 The IHR of the isolated SAN preparation was measured during steady-state spontaneous
 452 pacemaking under control conditions and during incrementing β -adrenergic stimulation for
 453 each of the 3 age groups. Data showed an age-associated reduction in basal intrinsic
 454 pacemaking (Figure 8A and summary in table 5) with intrinsic heart rate showing a linearly
 455 correlated reduction with age ($r^2 = 0.607$; $p = 0.0017$) falling from 274 ± 33 BPM at 6 months
 456 to 206 ± 19 BPM at 24 months of age. The EC50 to isoprenaline however remained
 457 unchanged with age (Figure 8A; 13.4 nM at 6 months and 13.7 nM at 24 months). At 1 μ M
 458 isoprenaline pacemaking differences were abolished across all age groups with intrinsic
 459 rates rising to 386 ± 36 and 368 ± 62 BPM in the youngest and oldest age groups
 460 respectively, indicating that a maximal response to the highest concentration of isoprenaline
 461 remains viable even in the SAN of the oldest rats that we studied.

462

463 **Table 5. Steady-state intrinsic heart rate (IHR) of isolated SAN with and without**

	6 months	12 months	24 months
IHR (beats per minute)	274 ± 33	256 ± 25	206 ± 19 *
Maximal Rate (1 μM Iso.)	386 ± 36 #	402 ± 22 #	368 ± 62 #
IHR in CPA	216 ± 26	204 ± 9	189 ± 27
Maximal Rate in CPA (1 μM Iso.)	258 ± 30	245 ± 22	240 ± 40

* $p=0.022$ comparing rate in 24-months with that at 6-months of age.

$p=<0.0001$ for rate in 1 μ M isoprenaline vs intrinsic heart rate in same age group.

464 **maximal β -adrenergic stimulation and/or cyclopiazonic acid (CPA) to block SERCA2A.**

465

466 To assess the functional involvement of the SR during β -adrenergic stimulation across the
 467 age groups, 3 μ M cyclopiazonic acid (CPA) was applied to inhibit SERCA2a and deplete the
 468 SR. CPA significantly reduced spontaneous activity at 6 and 12 months ($p = 0.023$ and
 469 0.044 respectively; RM-ANOVA) (Figure 8A and Table 5). Interestingly, in the oldest group of
 470 24 months of age CPA did not significantly reduce the basal intrinsic rate ($p = 0.904$).
 471 Intrinsic heart rate was no longer significantly different across the age groups in the
 472 presence of CPA ($p = 0.307$; RM-ANOVA; $n = 6$ in each group). CPA significantly reduced
 473 the response to isoprenaline in all age groups. In the presence of CPA the EC50 for
 474 isoprenaline did not significantly differ across age groups under control conditions or in the
 475 presence of CPA.

476

477 Activation maps for each sinoatrial node studied were constructed and the leading
478 pacemaker site located during the steady state response to each condition. Isoprenaline
479 caused a significant average shift in pacemaker location of 3.6 ± 1.6 mm ($p < 0.0001$, $n=6$ in
480 each group), Figure 8B. Application of CPA caused a small but significant shift in the leading
481 pacemaker site (1.2 ± 0.9 mm; $p = 0.0003$) and the significant isoprenaline-dependent shift in
482 the leading pacemaker site was maintained on subsequent application of isoprenaline in the
483 presence of CPA in all age groups (3.78 ± 1.6 mm; $p < 0.0001$). Comparing between age
484 groups there was no significant difference in pacemaker shift in response to isoprenaline,
485 CPA or the combination between age groups.

486

487 Examining the velocity of conduction between the leading pacemaker site and crista
488 terminalis under control conditions a significant reduction in conduction velocity was seen
489 across the SAN in the oldest group compared with tissue from the other two ages. Average
490 conduction velocity was 4.4 ± 0.25 m.sec⁻¹ at 6 months; 4.6 ± 0.60 m.sec⁻¹ at 12 months
491 falling significantly to 3.8 ± 0.23 m.sec⁻¹ at 24 months ($p = 0.041$ and 0.015 for 24 vs. 6
492 months and vs. 12 months respectively, $n = 6$ in each case).

493

494 A dose-dependent significant increase in conduction velocity in response to isoprenaline was
495 observed (Figure 8C) in all age groups with an average increase in velocity of 3.02 ± 1.07
496 m.sec⁻¹ ($p = <0.0001$) in the presence of 1 μ M isoprenaline. The magnitude of the increase
497 in velocity in response to isoprenaline differed significantly between all age groups, with the
498 largest increase seen in tissue from animals at 6 months of age where velocity increased by
499 5.1 ± 2.1 m.sec⁻¹ in response to 1 μ M isoprenaline, but 3.0 ± 1.1 m.sec⁻¹ for tissue from
500 animals at 12 months and 1.9 ± 0.5 m.sec⁻¹ for tissue from animals at 24 months ($p < 0.0001$
501 for 6 vs 24 months and $p = 0.001$ for 12 vs. 24 months).

502

503 CPA did not significantly impact conduction velocity under control conditions ($p = 0.989$) but
504 did abolish the significant impact of isoprenaline on conduction velocity in SAN tissue from
505 all age groups with the magnitude of increase in the presence of CPA falling to 1.25 ± 0.91
506 m.sec⁻¹; $p = 0.160$). In the presence of CPA there were no significant differences between
507 age groups in the response to isoprenaline.

508

509

510 **Figure 8 belongs here**

511

512

513 **Figure 8. Isoprenaline-dependent response of nodal function across the age groups**

514 **A**, Percentage change in intrinsic heart rate (beats per minute) (IHR) of the isolated SAN in
515 response to isoprenaline. The beating rate as determined in tissue from rats aged 6 months
516 under control conditions was taken as 100%. Upper traces show the % change (mean \pm
517 S.D.) for each age group in response to incremental doses of isoprenaline. Lower traces
518 show the effects of isoprenaline in the presence of 3 μ M CPA. **B**, magnitude of shift in the
519 leading pacemaker site on application of 1 μ M isoprenaline, 3 μ M CPA or the combination of
520 both. **C**, conduction velocity across the node from the leading pacemaker site to the crista
521 terminalis during application of different doses of isoprenaline alone or in the presence of 3
522 μ M CPA.

523 Discussion

524 The decline in maximal heart rate and increasing risk of pacemaker dysfunction is a
525 ubiquitous feature of ageing, as has been seen in many animal models and human studies
526 (Peters *et al.*, 2020). Previous work by ourselves and others have correlated this with
527 morphological changes of the SAN as well as changes in ion channel expression (Jones *et*
528 *al.*, 2004; Jones *et al.*, 2007; Monfredi & Boyett, 2015; Moghtadaei *et al.*, 2016). Alongside
529 this has been documented an altered response to adrenergic stimulation which may be
530 closely linked to an impaired ability of cAMP to modulate the 'calcium clock' component of
531 sinoatrial node pacemaking and so cause acceleration of the sinoatrial node (Liu *et al.*,
532 2014; Segal *et al.*, 2023). In this study we have investigated age-associated changes in key
533 components of cellular calcium regulation on pacemaking response as well as the effect of
534 entirely removing the SR contribution to pacemaking. The results reveal a sinoatrial node in
535 the elderly which operates at an intrinsically lower spontaneous frequency, but when the
536 calcium clock is disrupted age-associated differences in pacing rate and adrenergic
537 response are removed. The detailed mapping of protein changes and functional adaptations
538 identify a largely balanced scaling of changes with age preserving function and
539 responsiveness in the node but ultimately also show dysregulation of the 'calcium clock' may
540 underlie key age-associated changes in functional capacity, tolerance and response.

541

542 Right atria and ageing

543 Our male Wistar rat model showed that post-maturity with increasing age their body weight
544 increased significantly, as expected, but the heart weight did not change significantly with
545 age. Previous work in rats and other species, including humans have reported either no
546 change in heart weight simply with age, (Hindso *et al.*, 2017) or more commonly, age-
547 associated hypertrophy that may be secondary to hypertension and body mass increases
548 with age (Linzbach & Akuamoah-Boateng, 1973). Other studies have even indicated potential
549 reductions in cardiac mass relative to lean body mass in old age (Olivetti *et al.*, 1991), but
550 essentially it is the metabolically active tissue that is expected to be the key driver of cardiac
551 output.

552

553 Across our studies we have used the muscle-specific protein desmin to normalise our
554 western blot data, (Jones *et al.*, 2004; Jones *et al.*, 2007) as both mRNA and protein levels
555 of desmin do not change with age as shown in the rat atria (Table 4), whereas the
556 metabolically active protein Glyceraldehyde 3-phosphate dehydrogenase (GAPDH) showed
557 significant changes in levels of mRNA with increasing age within the RA (Table 3). Our initial
558 studies of calcium ion channels within the rat RA showed an age-associated significant

559 increase of $\text{Ca}_v1.3$ and $\text{Ca}_v3.1$ protein levels, and a significant decline in $\text{Ca}_v1.2$, whilst
560 $\text{Ca}_v1.2$ did not alter with age in the LA (Figures 2 & 3). Our key focus however has been the
561 SAN within the RA and age-related changes in calcium regulation that may be preponderant
562 there.

563

564 **Age-dependent changes in calcium regulators**

565 We show a significant loss of $\text{Ca}_v1.2$ channel protein from within the SAN of the rat during
566 advancing age. Such a change will potentially result in reduced excitability of the cells of the
567 node as well as reduced calcium-loading of the SR, potentially limiting the ability of the SR to
568 modulate pacemaking via the calcium clock. These channels are key for the upstroke of the
569 action potential in SAN myocytes once threshold is reached but also serve to service the
570 calcium loading of the cell, thus directly modulate functioning of the 'calcium clock' as well as
571 the funny current I_f indirectly (Hagiwara & Irisawa, 1989). Of considerable interest is the
572 observed shift in association between pharmacological modulation of the current through
573 $\text{Ca}_v1.2$ using nifedipine and the ensuing impact on heart rate. Whilst the EC50 does not shift,
574 implying the interaction with the channel in terms of binding is conserved, the four-fold shift
575 on the Hill coefficient indicates a notable change in the relationship between the current and
576 pacemaking. The elevated sensitivity may in part be simply due to the overall drop in
577 channel density but also reflects a shift in the links between membrane calcium flux via
578 $\text{Ca}_v1.2$ and pacemaking. The relationship between pacemaking and this flux is complex to
579 assess since this acts as a depolarising influence but also critically a key loading flux for the
580 SR, which we see is also altering in influence in old age, together with other elements that
581 ensure calcium balance such as NCX. The steep sensitivity implies a reduced capacity to
582 deal with flux variation and still maintain calcium balance within a suitable range to ensure
583 continued stable pacemaking. In the face of an already reduced inward calcium flux and in
584 tandem with reduced SR function the node experiences a steep reduction in potential
585 depolarising current from both the calcium current and SR calcium releases, with the net
586 impact observed here.

587

588 **Age and changes in the balance of 'calcium clock' components**

589 Analysing the components of the SAN calcium clock we see broad depression in the
590 expression of all elements associated directly with the sarcoplasmic reticulum and its
591 function. Calcium release and uptake proteins are reduced by a similar magnitude in old
592 age indicating possible co-regulation to ensure maintained equilibria essential for continued
593 stable function, since cumulative imbalance of calcium flux will rapidly lead to arrhythmias or
594 cell death. SERCA2a is key for maintaining loading of the SR with calcium and is a key
595 controller of diastolic calcium in partnership with calcium entry via the L-type calcium

596 channel. Modulating this relationship is the influx of calcium, and the activity of SERCA2
597 modulated by PLB in response to production of cAMP triggered by adrenergic stimulation
598 (Capel & Terrar, 2015). SERCA, RYR and PLB all fell proportionately in old age maintaining
599 this control equilibrium and perhaps more indicative of a general loss in SR density rather
600 than shifting control. As a potential means to ensure maintained calcium balance, even
601 though L-type calcium channel expression is also falling, NCX rises. As such in old age the
602 scope for calcium release from the SR to dynamically respond to pacemaking is likely to be
603 suppressed, although the elevated NCX may be sufficient to facilitate the basal contribution
604 of depolarising current secondary to SR release (Groenke *et al.*, 2013) which is potentially
605 occurring at a reduced density. Previous work in an over-expressor model of NCX showed
606 elevations in NCX to be capable of increasing the dynamic response to adrenergic
607 stimulation (Kaese *et al.*, 2017). Here we do not see such an enhancement but the elevation
608 in NCX is certainly likely to be key in maintaining the response we do see in the face of a
609 falling potential SR component driving pacemaking.

610

611 **Impact of stopping the ‘calcium clock’ leaving the membrane one to run the beat**

612 The key role of the calcium clock in regulating the SAN is seen when we effectively remove
613 the function of the SR using CPA to inhibit SERCA function. This only impacted basal
614 pacemaking of the SAN significantly in tissue from the younger groups. In contrast, CPA had
615 insignificant impact on SAN activity in tissue from elderly animals indicating a key shift in the
616 influence of the calcium clock on activity of the node. One surprising observation is that
617 despite the apparent lack of a role for the SR in maintaining the pacemaker rate at baseline
618 in the old animals they do show an apparently normal dose-response to isoprenaline with a
619 maintained EC50, and this response remains comparable between age groups in the
620 presence of CPA. The implication is that the signal transduction processes responsible for
621 the adrenergic response remain perfectly functional in old age. We haven’t looked in detail at
622 each part of the signal transduction process, but other studies have similarly found
623 preserved potential for response (Liu *et al.*, 2014) even though kinetics and sensitivity may
624 be subtly altered at various stages of the process from catecholamine interaction with
625 receptors through to cAMP generation (Xiao *et al.*, 1998) and equilibrium with
626 phosphodiesterases (Yaniv *et al.*, 2016). Despite this preserved potential for response in the
627 isolated SAN, maximal heart rate in the intact organism is depressed with age indicating key
628 aspects such as neural input and metabolic regulation which may be differentially modulated
629 or limited in the intact organism may be key for developing our understanding of why peak
630 heart rate is suppressed in the elderly.

631

632 A key observation is that with SR function suppressed the response to isoprenaline at all ages
633 becomes equivalent, although much depressed in range. Thus, it seems in the male rat at
634 least, modulation of If by cAMP is insufficient alone to drive a normal full pacemaker
635 response to adrenergic input. The ~70% reduction in dynamic response to isoprenaline seen
636 in the SAN with SERCA inhibition present suggests, in the rat at least, activation of HCN and
637 the membrane clock can only achieve ~30% of the normal increase in activation frequency.
638 This balance in dynamic response seems preserved across the age range even though
639 basal activity is suppressed in SAN tissue from the oldest animals we studied again implying
640 balanced regulation across the age range rather than identifying a distinct imbalance arising
641 that can be targeted to reduce the impact of ageing.

642

643 **Impact on pacemaker response and conduction**

644 We have conducted our experiments using the intact functioning SAN. A key regulator of
645 pacemaker activity isn't just seen at the individual cell level since the activation of the node
646 and its ability to drive the pacing of the heart is dependent on the electrotonic interactions
647 between cells of the leading pacemaker site and surrounding tissue. Changes in pacemaker
648 frequency are commonly associated with shifts in dominant pacemaker location and
649 propagation of activation across the tissue. At its most extreme there are suggestions that in
650 some species, including humans, distinct foci for pacemaking depending on frequency may
651 exist (Brennan *et al.*, 2020) representing areas with differing expression of ion channels
652 and/or electrotonic interaction with the surrounding tissue modulated by frequency and
653 focussed autonomic influence. In the isolated nodal preparations, we have used we do not
654 have focussed autonomic input, but we did still see significant shifts in the location of the
655 leading pacemaker site when isoprenaline was applied, even when SR function was
656 inhibited with CPA. This shift was preserved across all age groups. Despite a significant shift
657 in basal pacemaker frequency in tissue from the younger ages studied, no shift in
658 pacemaker location was however observed when SR function was inhibited with CPA. This
659 observation raises questions regarding what may drive pacemaker shift. If shifts in calcium
660 balance and even depolarisation frequency, of the magnitudes we have seen with age and
661 CPA are not enough to cause pacemaker shift then maybe this may represent simply a
662 difference in density of expression of adrenergic receptors or other elements of the
663 transduction machinery for actioning the adrenergic response. A surprising observation was
664 the shift in conduction velocity across the node with isoprenaline. An increase in conduction
665 velocity is expected as the upstroke velocity and amplitude of the action potential is
666 increased with adrenergic stimulation, but this was only observed in nodal tissue from the
667 younger animals. The failure of isoprenaline to be able to increase conduction velocity in the
668 oldest group may be indicative of the loss of calcium channels impacting the upstroke of the

669 action potential, or equally may reflect loss of connexins key to permit rapid electrical
670 propagation (Jones *et al.*, 2001). Irrespective of the reason, this data indicates a limitation for
671 supporting stable higher-frequency activation of the node and surrounding tissue due to
672 limits in the rate at which the activation can spread to the atria. This has the potential to be a
673 key issue for the development of sick-sinus syndrome and atrial fibrillation, although future
674 work making more-detailed sub-regional analysis all across the node is required to clearly
675 identify how this failure of conduction is arising.

676

677 **Clinical Implications and Implications for Human Ageing**

678 The identified shifts in calcium regulatory processes, baseline pacemaker rate as well as
679 suppressed ability to enhance conduction velocity are all key issues to consider in the
680 perspective of the aged human heart. Calcium channel blockers such as verapamil are still
681 used widely, chiefly for their impact on vascular function but the changing relationship
682 between calcium balance and pacemaker function does indicate a developing danger.
683 Indeed use of verapamil in patients with sick sinus syndrome has previously been noticed to
684 have four to five times the impact on SAN function as when applied in control individuals, a
685 comparable magnitude of shift as our identified shift in slope of the response of the isolated
686 rat SAN to calcium channel block (Carrasco *et al.*, 1978). The obvious clinical implication of
687 this is to use calcium channel modulators with considerable caution in the elderly, paying
688 careful attention to the potential for inducing and exacerbating sick-sinus syndrome.

689

690 In the light of broader human ageing the implications remain that until we can solve the issue
691 of the continued drop in SAN function and peak heart rate with age we cannot expect to be
692 able to significantly prolong maximal lifespan without encountering pacemaker problems.
693 Solutions do not appear to simply lie in restoring response to adrenergic stimulation, but
694 instead are likely to require maintenance or restoration of key aspects determining
695 conduction through the SAN and capacity within the calcium regulatory processes,
696 membrane and SR associated, to ensure stable response and continued activity at suitable
697 rates to meet requirements for adequate cardiac output.

698

699 **Limitations and Future Work**

700 One interesting feature of our findings was we did not see a significantly limited response to
701 isoprenaline in aged tissue as generally reported by others in the intact heart and other
702 preparations (Lakatta *et al.*, 1975). In other cases, what has often been seen is a shift in the
703 dose-response curve to adrenergic stimuli whilst direct elevations of cAMP or saturating
704 doses of agonists show maximal responses are in fact preserved (as seen here and for
705 example by Liu *et al.* (Liu *et al.*, 2014). As such *in-vivo* a depressed maximal rate is

706 common, but ex-vivo any differences in signal transduction arising from alterations to
707 autonomic input or accumulation of agonists it would appear can be negated. The implication
708 is that the end effector of heart rate elevation the peak rate of nodal depolarisation remains
709 capable of a full range of function in advanced age, so to identify the source of depressed
710 response we need to look to manipulate the signal transduction pathway if we wish to
711 restore youthful function. Having said this, we do see signs of potential for greater instability
712 due to the changing balance of components regulating intracellular calcium buffering. Future
713 experiments will aim to assess this more directly but also identify steps on the signalling
714 pathway that alter the relationship between cAMP production and activation of the integrated
715 pacemaking mechanism of the calcium and membrane clocks in advanced age. A key
716 feature to permit stable restoration of higher pacemaker rats to the aged SAN though would
717 also appear to be modulation of conduction.

718

719 One limitation in translating these findings to the human condition is understanding that the
720 shifts in impact of differing mechanisms of pacemaker modulation and atrial excitability will
721 vary between species and also ages. For example, in humans, the resting heart rate is
722 normally kept reduced by parasympathetic input and on removing this and observing the
723 intrinsic rhythm an acceleration is seen (Christou & Seals, 2008). In others, such as the rat
724 as we have studied here, the resting heart rate *in vivo* is maintained by tonic sympathetic
725 input and on removing this the intrinsic rate is, in contrast to humans, lower than that seen *in*
726 *vivo* (Di Gennaro *et al.*, 1987). This latter response may also apply to the aged human heart
727 (Christou & Seals, 2008), potentially making the rat heart more in-line with the aged human
728 heart. These indicate a differing role for tonic sympathetic drive across ages and species
729 which will go hand-in-hand with associated signal transduction, response and the role of
730 pacemaker mechanisms in facilitating the dynamic response of the heartbeat. Further
731 experiments on human tissue are required to refine our understanding of the relative impact
732 of the membrane and calcium clocks across the SAN and how each are modulated by
733 adrenergic stimulation and age.

734

735 **Conclusion**

736 In conclusion, our data shows a changing relationship between pacemaker function and
737 cellular calcium handling with advancing age. Whilst the identified changes also show
738 preservation of a good level of calcium handling function and response to isoprenaline, there
739 are indicators of an increased risk of instability and altered responses to physiological and
740 pharmacological interventions. Pharmacological agents modulating the changing dynamics
741 driving the SAN activity are routinely administered in treatment of hypertension for example,

742 however due to an increasing risk of precipitating sinus node dysfunction greater care is
 743 needed in consideration of their use in elderly patients.

744

745

746

747 **Additional Information**

748 All authors declare there are no competing interests or conflicts of interest.

749 AI was not used to generate any content for this manuscript.

750 Drs Godbeer, Jones and Lancaster contributed to the data collection process and analysis.

751 Manuscript drafting, editing and further data analysis was conducted by Drs Jones and
 752 Lancaster.

753 Data Availability Statement: Raw data for activity responses shown in Figures 4 and 8 are
 754 available as online Supporting Information.

755

756 **Acknowledgements**

757 Thanks to Dr Jenny Waby for her expertise and assistance to Dr Godbeer in desmin mRNA
 758 analysis. Dr Godbeer (née Hatch) thanks the University of Hull for her PhD studentship (no
 759 grant code).

760

761 **References**

762 Bers D & Lakatta EG. (2023). What makes the sinoatrial node tick? A question not for the
 763 faint of heart. *Philos Trans R Soc Lond B Biol Sci* **378**, 20220180.

764

765 Brennan JA, Chen Q, Gams A, Dyavanapalli J, Mendelowitz D, Peng W & Efimov IR. (2020).
 766 Evidence of Superior and Inferior Sinoatrial Nodes in the Mammalian Heart. *JACC*
 767 *Clin Electrophysiol* **6**, 1827-1840.

768

769 Burdett P & Lip GYH. (2022). Atrial fibrillation in the UK: predicting costs of an emerging
 770 epidemic recognizing and forecasting the cost drivers of atrial fibrillation-related
 771 costs. *Eur Heart J Qual Care Clin Outcomes* **8**, 187-194.

772

773 Capel RA & Terrar DA. (2015). The importance of Ca(2+)-dependent mechanisms for the
 774 initiation of the heartbeat. *Front Physiol* **6**, 80.

775

776 Carrasco HA, Fuenmayor A, Barboza JS & Gonzalez G. (1978). Effect of verapamil on
 777 normal sinoatrial node function and on sick sinus syndrome. *Am Heart J* **96**, 760-771.

778

779 Christou DD & Seals DR. (2008). Decreased maximal heart rate with aging is related to
 780 reduced β -adrenergic responsiveness but is largely explained by a reduction in
 781 intrinsic heart rate. *Journal of applied physiology (Bethesda, Md : 1985)* **105**, 24-29.

782

783 Di Gennaro M, Bernabei R, Sgadari A, Carosella L & Carbonin PU. (1987). Age-related
 784 differences in isolated rat sinus node function. *Basic Research in Cardiology* **82**, 530-
 785 536.

786
 787 Fang MC, Chen J & Rich MW. (2007). Atrial fibrillation in the elderly. *The American journal of*
 788 *medicine* **120**, 481-487.

789
 790 Fleg JL, Morrell CH, Bos AG, Brant LJ, Talbot LA, Wright JG & Lakatta EG. (2005).
 791 Accelerated longitudinal decline of aerobic capacity in healthy older adults.
 792 *Circulation* **112**, 674-682.

793
 794 Groenke S, Larson ED, Alber S, Zhang R, Lamp ST, Ren X, Nakano H, Jordan MC,
 795 Karagueuzian HS, Roos KP, Nakano A, Proenza C, Philipson KD & Goldhaber JI.
 796 (2013). Complete atrial-specific knockout of sodium-calcium exchange eliminates
 797 sinoatrial node pacemaker activity. *PLoS One* **8**, e81633.

798
 799 Hagiwara N & Irisawa H. (1989). Modulation by intracellular Ca²⁺ of the hyperpolarization-
 800 activated inward current in rabbit single sino-atrial node cells. *J Physiol* **409**, 121-141.

801
 802 Hindso L, Fuchs A, Kuhl JT, Nilsson EJ, Sigvardsen PE, Kober L, Nordestgaard BG &
 803 Kofoed KF. (2017). Normal values of regional left ventricular myocardial thickness,
 804 mass and distribution-assessed by 320-detector computed tomography angiography
 805 in the Copenhagen General Population Study. *Int J Cardiovasc Imaging* **33**, 421-429.

806
 807 Jones SA, Boyett MR & Lancaster MK. (2007). Declining into failure: the age-dependent loss
 808 of the L-type calcium channel within the sinoatrial node. *Circulation* **115**, 1183-1190.

809
 810 Jones SA, Lancaster MK & Boyett MR. (2001). Age-associated disappearance of
 811 connexin43 within the sinoatrial node. *Circulation* **104**, 643.

812
 813 Jones SA, Lancaster MK & Boyett MR. (2004). Ageing-related changes of connexins and
 814 conduction within the sinoatrial node. *J Physiol* **560**, 429-437.

815
 816 Kaese S, Boge Holz N, Pauls P, Dechering D, Olligs J, Kolker K, Badawi S, Frommeyer G,
 817 Pott C & Eckardt L. (2017). Increased sodium/calcium exchanger activity enhances
 818 beta-adrenergic-mediated increase in heart rate: Whole-heart study in a homozygous
 819 sodium/calcium exchanger overexpressor mouse model. *Heart Rhythm* **14**, 1247-
 820 1253.

821
 822 Keller KM & Howlett SE. (2016). Sex Differences in the Biology and Pathology of the Aging
 823 Heart. *The Canadian journal of cardiology* **32**, 1065-1073.

824
 825 Lakatta EG, Gerstenblith G, Angell CS, Shock NW & Weisfeldt ML. (1975). Diminished
 826 inotropic response of aged myocardium to catecholamines. *Circ Res* **36**, 262-269.

827
 828 Linzbach AJ & Akuamoah-Boateng E. (1973). [Changes in the aging human heart. I. Heart
 829 weight in the aged]. *Klin Wochenschr* **51**, 156-163.

830
 831 Liu J, Sirenko S, Juhaszova M, Sollott SJ, Shukla S, Yaniv Y & Lakatta EG. (2014). Age-
 832 associated abnormalities of intrinsic automaticity of sinoatrial nodal cells are linked to
 833 deficient cAMP-PKA-Ca²⁺ signaling. *Am J Physiol Heart Circ Physiol* **306**, H1385-
 834 1397.

835
 836 MacLennan DH & Kranias EG. (2003). Phospholamban: a crucial regulator of cardiac
 837 contractility. *Nat Rev Mol Cell Biol* **4**, 566-577.

838

839 Moghtadaei M, Jansen HJ, Mackasey M, Rafferty SA, Bogachev O, Sapp JL, Howlett SE &
840 Rose RA. (2016). The impacts of age and frailty on heart rate and sinoatrial node
841 function. *J Physiol* **594**, 7105-7126.

842

843 Monfredi O & Boyett MR. (2015). Sick sinus syndrome and atrial fibrillation in older persons -
844 A view from the sinoatrial nodal myocyte. *J Mol Cell Cardiol* **83**, 88-100.

845

846 Olivetti G, Melissari M, Capasso JM & Anversa P. (1991). Cardiomyopathy of the aging
847 human heart. Myocyte loss and reactive cellular hypertrophy. *Circ Res* **68**, 1560-
848 1568.

849

850 ONS. (2025). National population projections: 2022-based. Office for National Statistics UK,
851 UK.

852

853 Peters CH, Sharpe EJ & Proenza C. (2020). Cardiac Pacemaker Activity and Aging. *Annu
854 Rev Physiol* **82**, 21-43.

855

856 Segal S, Shemla O, Shapira R, Peretz NK, Lukyanenko Y, Brosh I, Behar J, Lakatta EG,
857 Tsutsui K & Yaniv Y. (2023). cAMP signaling affects age-associated deterioration of
858 pacemaker beating interval dynamics. *Geroscience* **45**, 2589-2600.

859

860 Tsutsui K, Monfredi OJ, Sirenko-Tagirova SG, Maltseva LA, Bychkov R, Kim MS, Ziman BD,
861 Tarasov KV, Tarasova YS, Zhang J, Wang M, Maltsev AV, Brennan JA, Efimov IR,
862 Stern MD, Maltsev VA & Lakatta EG. (2018). A coupled-clock system drives the
863 automaticity of human sinoatrial nodal pacemaker cells. *Sci Signal* **11**:eaap7608.

864

865 Turner MJ, Mier CM, Spina RJ, Schechtman KB & Ehsani AA. (1999). Effects of age and
866 gender on the cardiovascular responses to isoproterenol. *The journals of gerontology
867 Series A, Biological sciences and medical sciences* **54**, B393-400; discussion B401-
868 393.

869

870 Xiao RP, Tomhave ED, Wang DJ, Ji X, Boluyt MO, Cheng H, Lakatta EG & Koch WJ.
871 (1998). Age-associated reductions in cardiac beta1- and beta2-adrenergic responses
872 without changes in inhibitory G proteins or receptor kinases. *The Journal of clinical
873 investigation* **101**, 1273-1282.

874

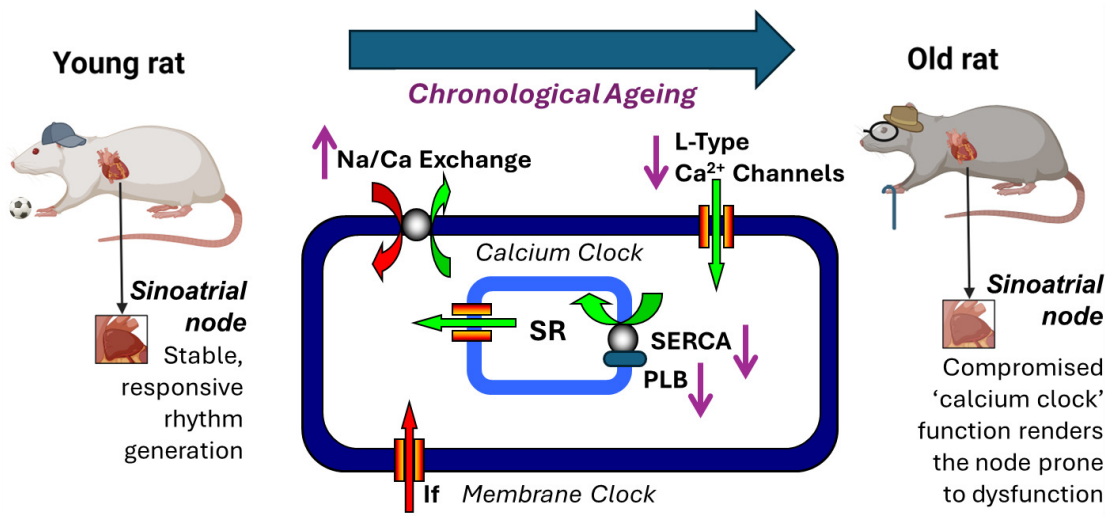
875 Yaniv Y, Ahmet I, Tsutsui K, Behar J, Moen JM, Okamoto Y, Guiriba TR, Liu J, Bychkov R &
876 Lakatta EG. (2016). Deterioration of autonomic neuronal receptor signaling and
877 mechanisms intrinsic to heart pacemaker cells contribute to age-associated
878 alterations in heart rate variability in vivo. *Aging Cell* **15**, 716-724.

879

880 Yue X, Hazan A, Lotteau S, Zhang R, Torrente AG, Philipson KD, Ottolia M & Goldhaber JI.
881 (2020). Na/Ca exchange in the atrium: Role in sinoatrial node pacemaking and
882 excitation-contraction coupling. *Cell Calcium* **87**, 102167.

883

884



Created in BioRender.com 

Abstract figure

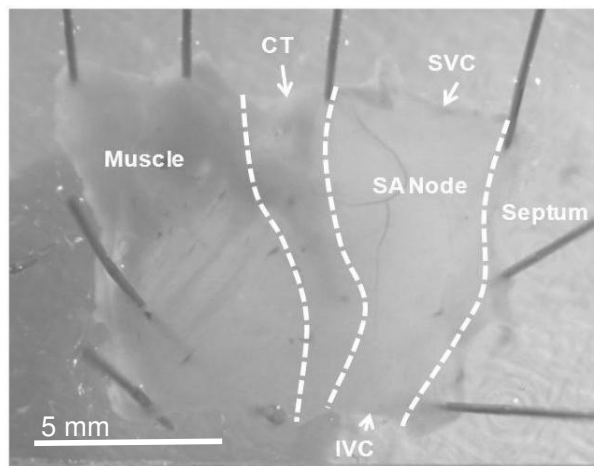


Figure 1. Endocardial surface of the right atria

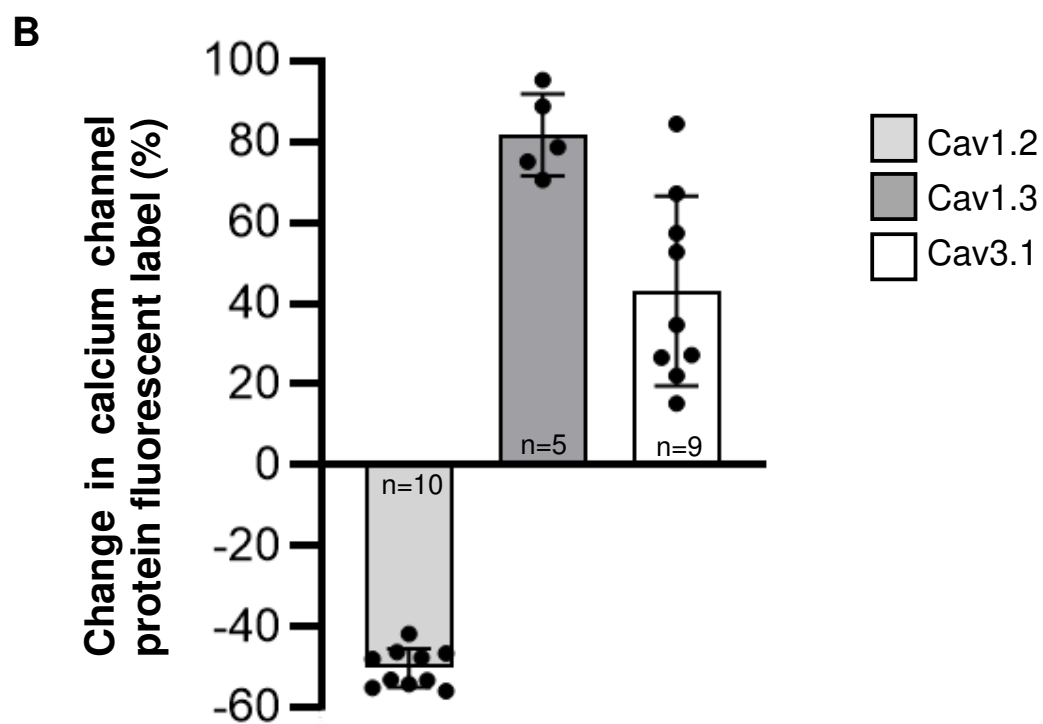
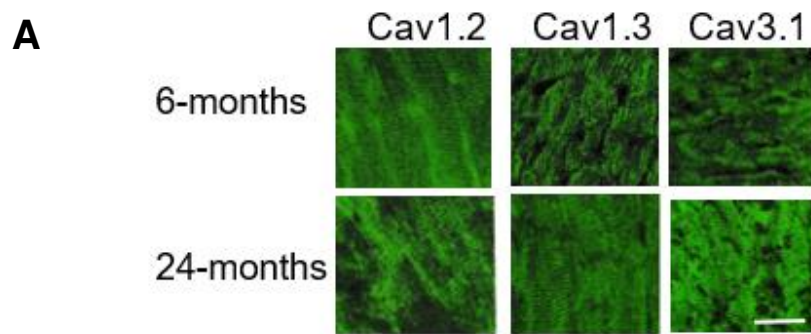


Figure 2. Changes in IHC calcium channel label within RA at 24-months of age.

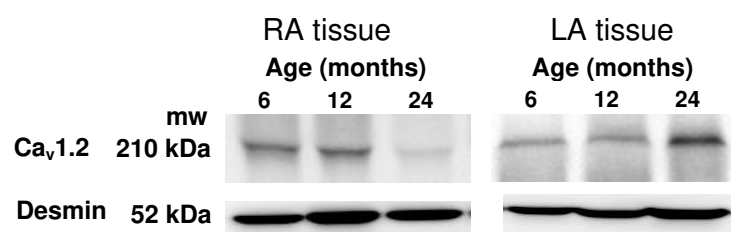
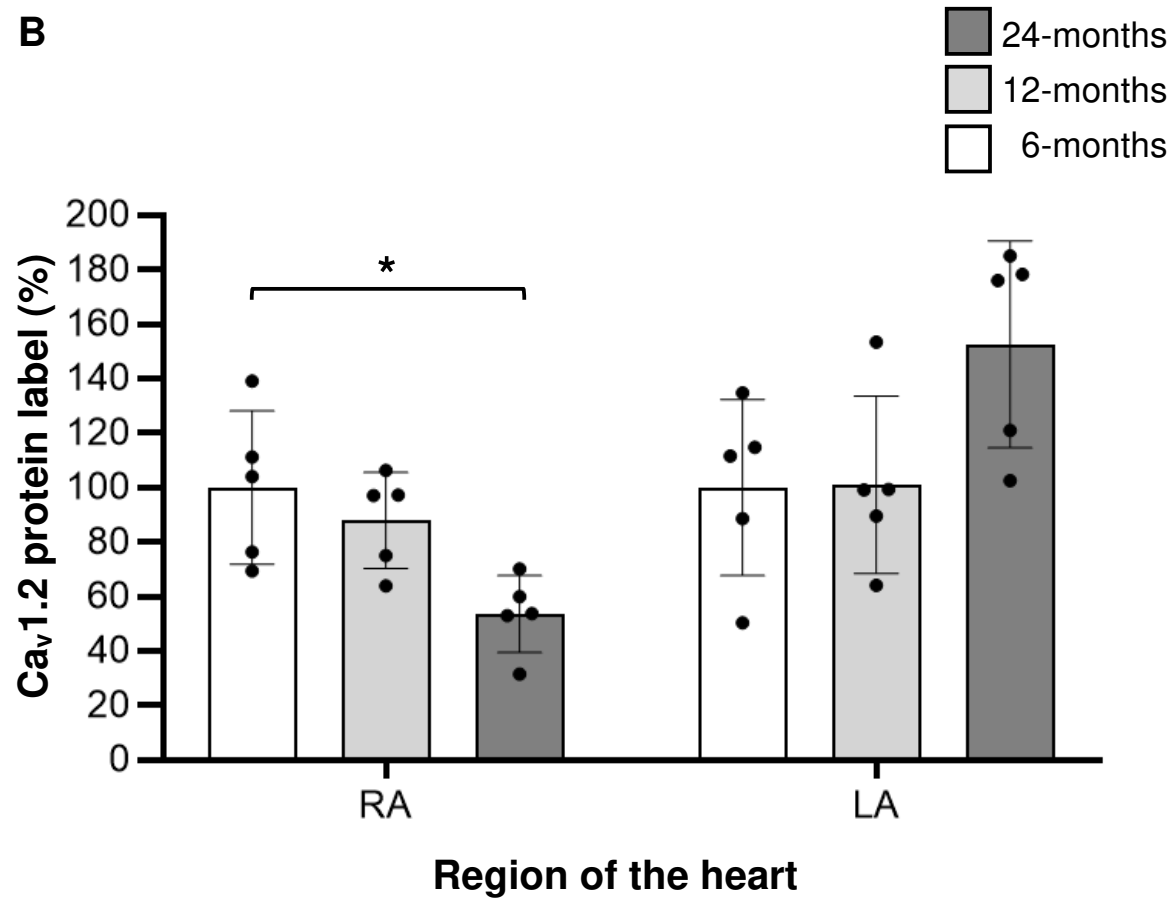
A**B**

Figure 3. Age-associated changes of $\text{Ca}_v1.2$ protein across the atria.

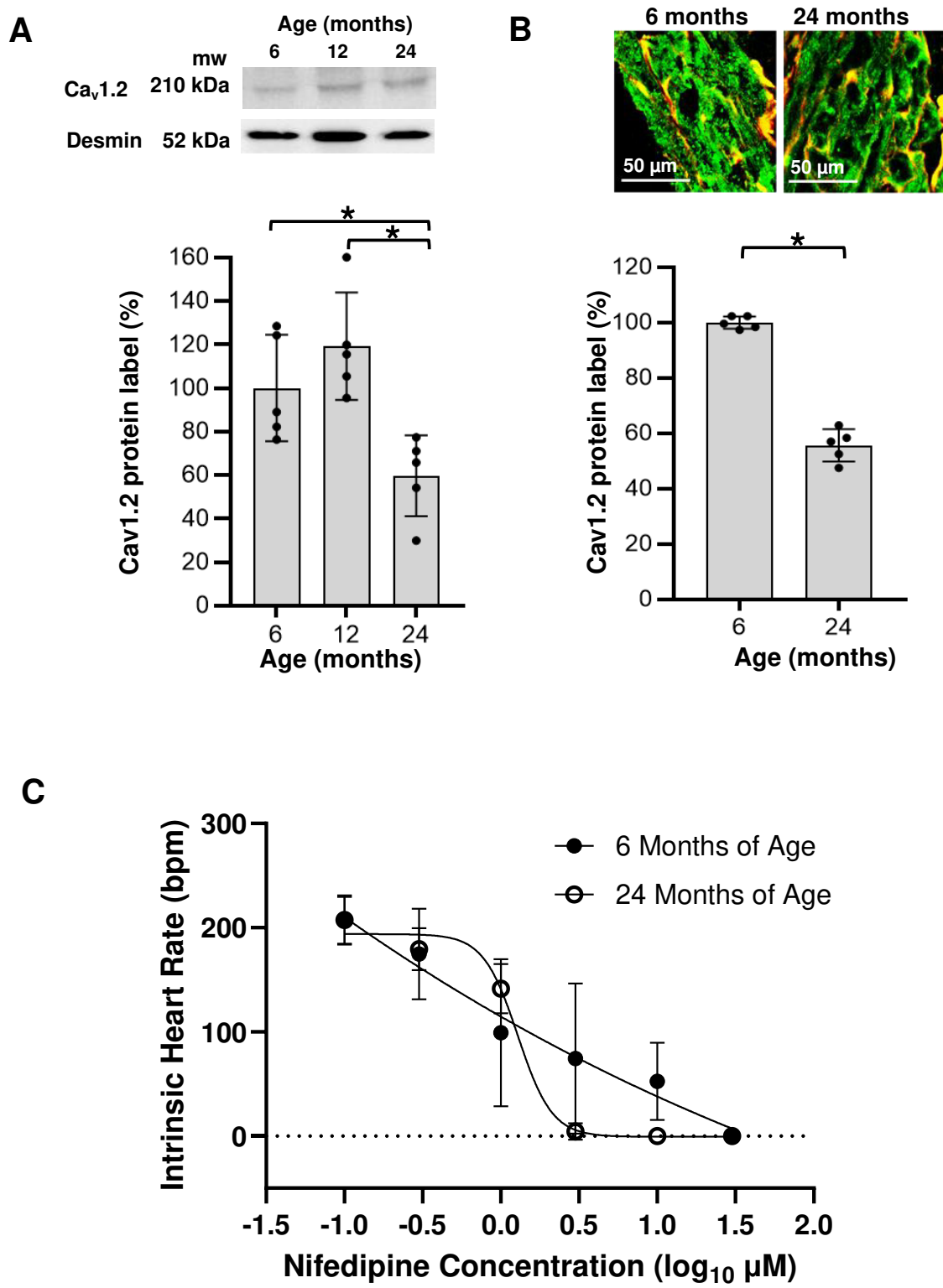


Figure 4. Age-associated changes of $\text{Ca}_v1.2$ protein and activity within the SAN.

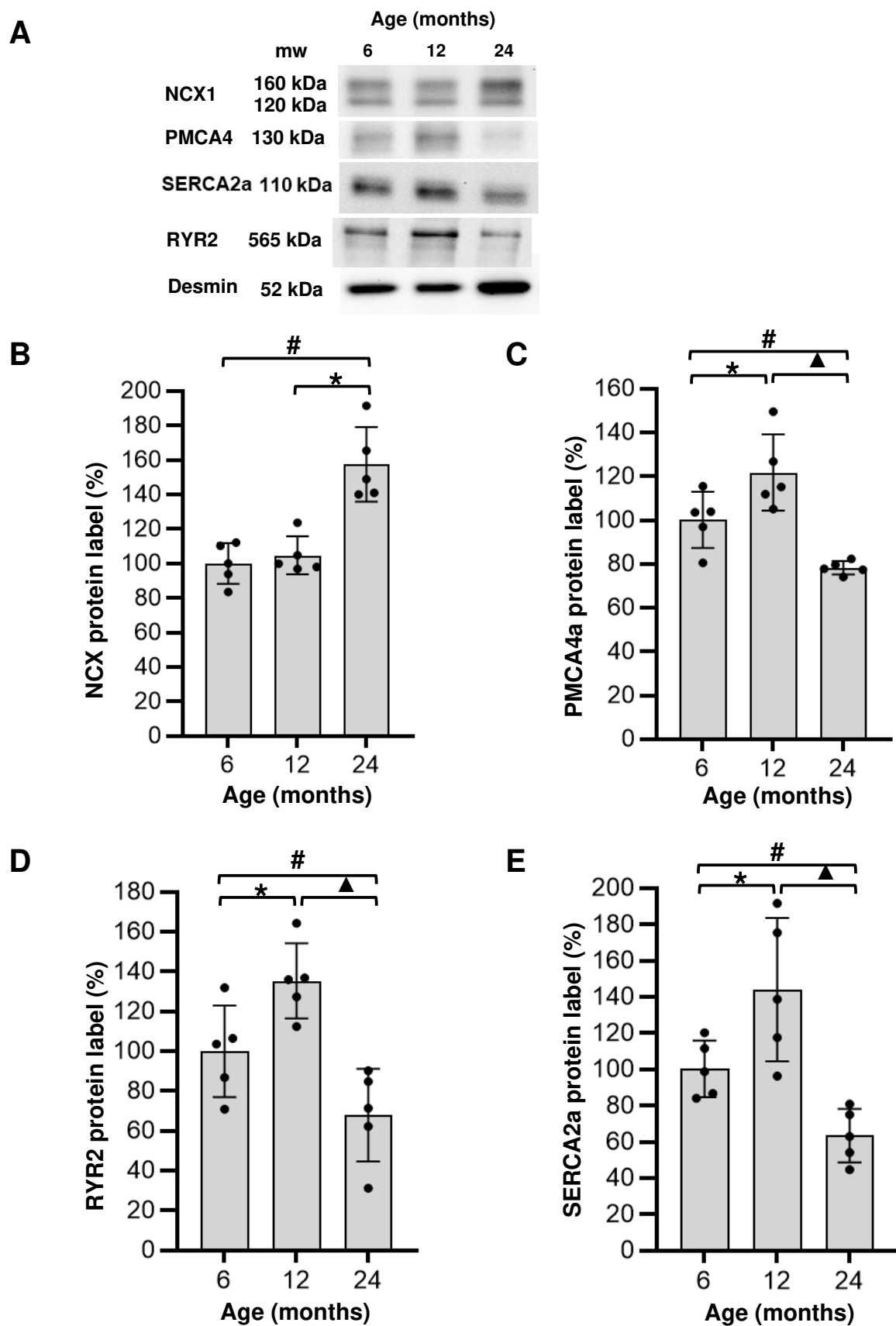


Figure 5. Effect of ageing on levels of calcium handling proteins expressed in the sinoatrial node.

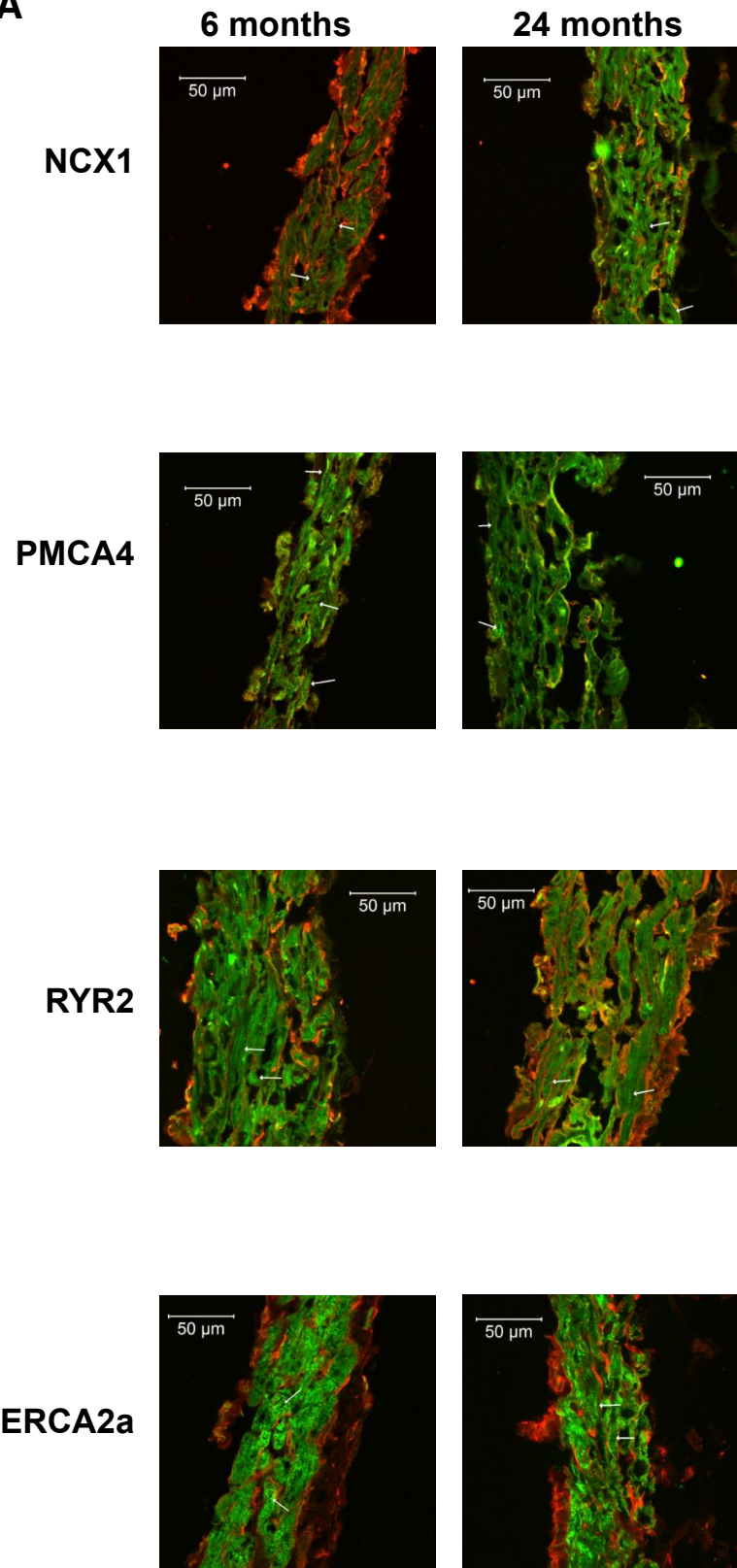
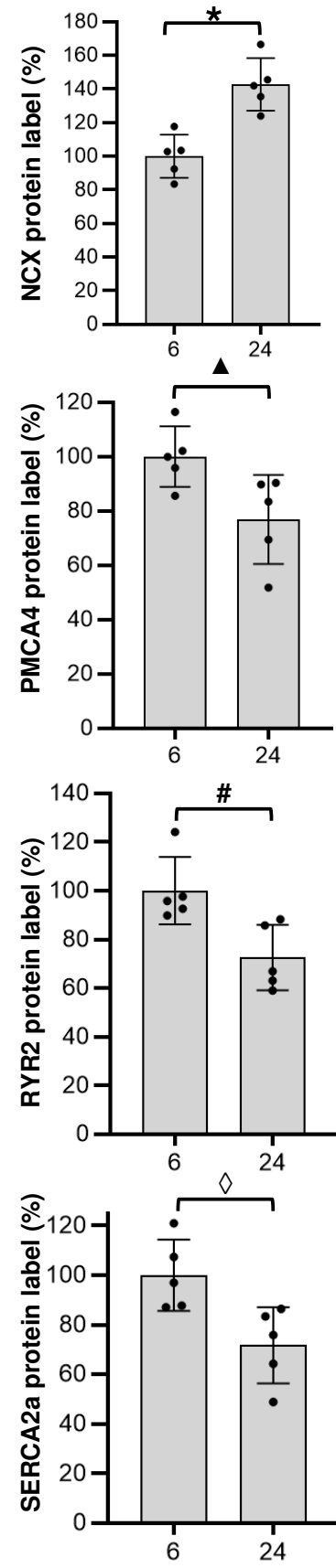
A**B**

Figure continues on next page

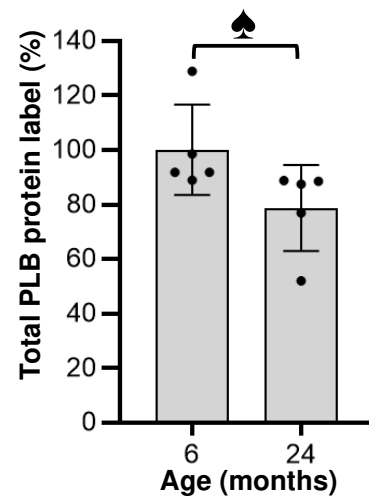
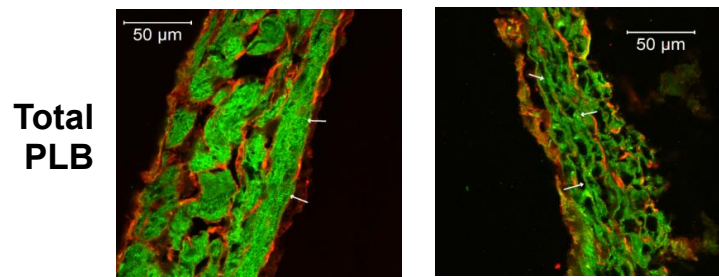


Figure 6. Age-dependent changes of proteins labelled within the sinoatrial region.

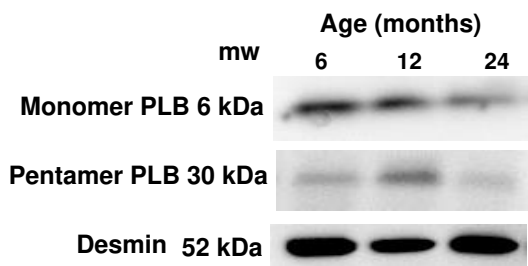
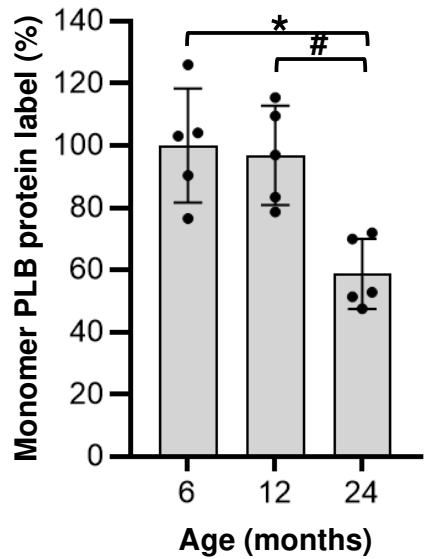
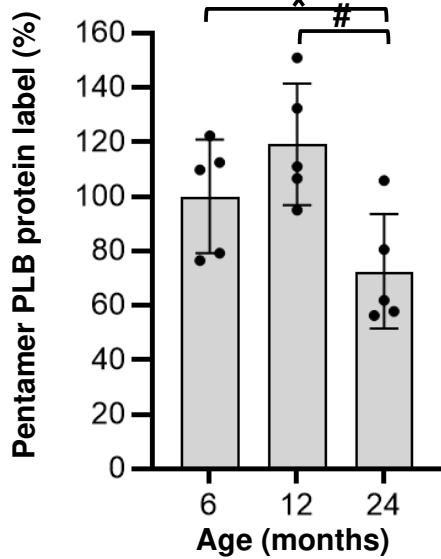
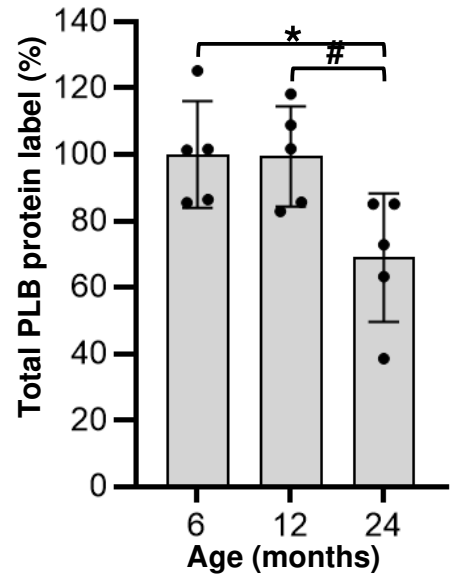
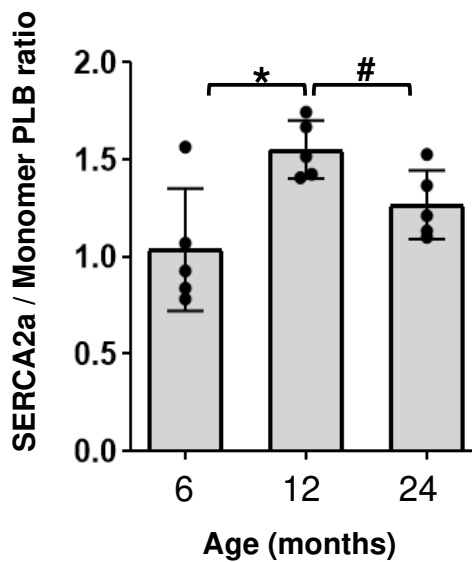
A**B****C****D****E**

Figure 7. Age-dependent protein expression changes of phospholamban in the sinoatrial node.

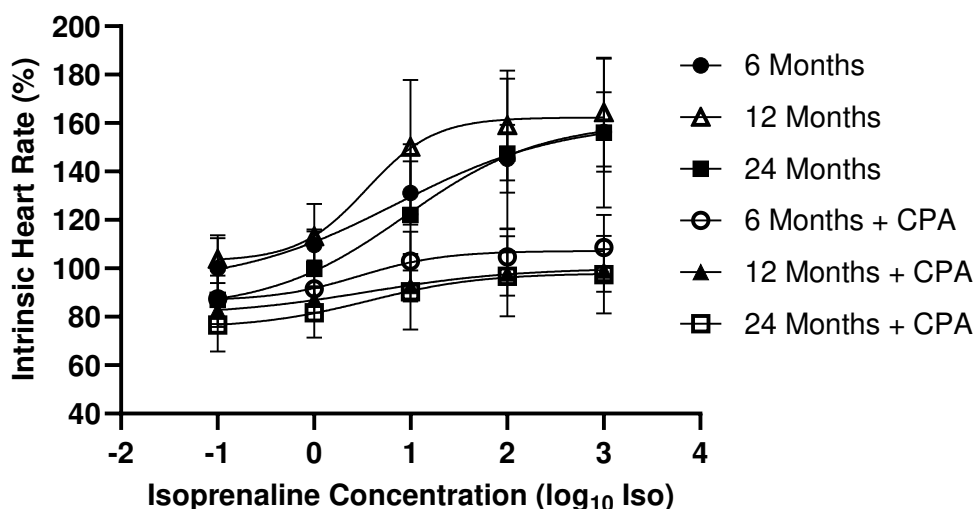
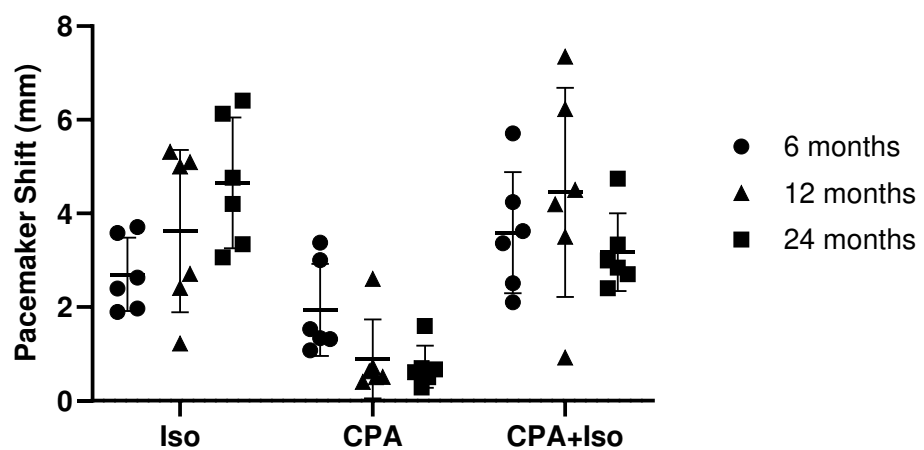
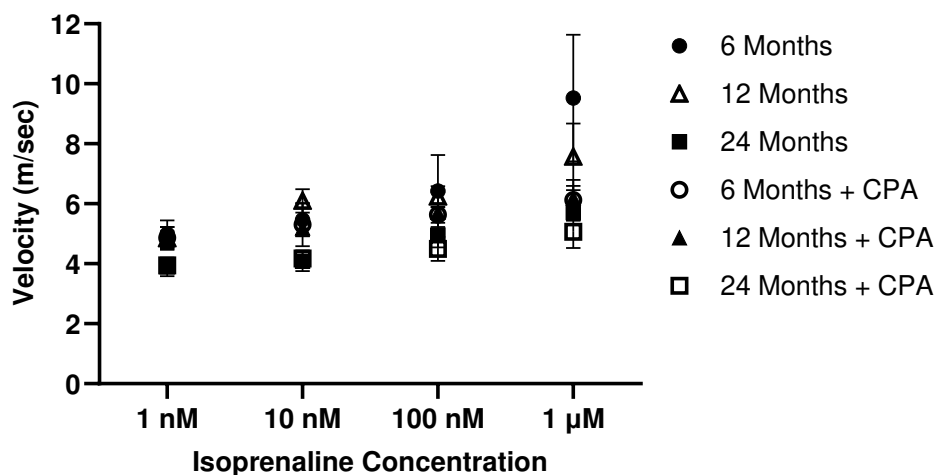
A**B****C**

Figure 8. Isoprenaline-dependent response of nodal function across the age groups